JOURNAL OF VIROLOGY, Mar. 2007, p. 2391–2400 Vol. 81, No. 5
0022-538X/07/$08.00+0 doi:10.1128/JVI.01601-06

Inhibition of Filovirus Replication by the Zinc Finger Antiviral Protein[▽]

Stefanie Müller,[1]† Peggy Möller,[2]† Matthew J. Bick,[1]‡ Stephanie Wurr,[1] Stephan Becker,[2]§ Stephan Günther,[1] and Beate M. Kümmerer[1]*

Department of Virology, Bernhard-Nocht-Institute for Tropical Medicine, 20359 Hamburg, Germany,[1] and Institute of Virology, Philipps University Marburg, 35043 Marburg, Germany[2]

Received 26 July 2006/Accepted 7 December 2006

The zinc finger antiviral protein (ZAP) was recently shown to inhibit Moloney murine leukemia virus and Sindbis virus replication. We tested whether ZAP also acts against Ebola virus (EBOV) and Marburg virus (MARV). Antiviral effects were observed after infection of cells expressing the N-terminal part of ZAP fused to the product of the zeocin resistance gene (NZAP-Zeo) as well as after infection of cells inducibly expressing full-length ZAP. EBOV was inhibited by up to 4 log units, whereas MARV was inhibited between 1 to 2 log units. The activity of ZAP was dependent on the integrity of the second and fourth zinc finger motif, as tested with cell lines expressing NZAP-Zeo mutants. Heterologous expression of EBOV- and MARV-specific sequences fused to a reporter gene suggest that ZAP specifically targets L gene sequences. The activity of NZAP-Zeo in this assay was also dependent on the integrity of the second and fourth zinc finger motif. Time-course experiments with infectious EBOV showed that ZAP reduces the level of L mRNA before the level of genomic or antigenomic RNA is affected. Transient expression of ZAP decreased the activity of an EBOV replicon system by up to 95%. This inhibitory effect could be partially compensated for by overexpression of L protein. In conclusion, the data demonstrate that ZAP exhibits antiviral activity against filoviruses, presumably by decreasing the level of viral mRNA.

Ebola virus (EBOV) and Marburg virus (MARV) belong to the family *Filoviridae*. Their genome consists of a single-stranded RNA genome of negative polarity with a length of about 19 kb. The filovirus genome is transcribed in monocistronic mRNA species, which encode seven structural proteins: a single surface protein (GP), a matrix protein (virus protein 40 [VP40]), a second minor matrix protein (VP24), and four nucleocapsid proteins (nucleoprotein [NP], L protein, VP35, and VP30) (7, 15, 16, 18, 25). Both EBOV and MARV cause severe hemorrhagic fever in humans and nonhuman primates (4, 19). Infections with filoviruses are characterized by high fever, hemorrhages, and shock (19, 22). For Zaire-EBOV and MARV, mortality rates up to 90% have been described; the mortality rates for Sudan-EBOV are about 60% (from the Centers for Disease Control and Prevention website [http://www.cdc.gov/]). To date, neither a vaccine nor a therapy for treating infected patients is available.

In contrast to many other viruses, no host cell proteins with antiviral activity have been identified so far for filoviruses. However, it is known that filoviruses antagonize the interferon (IFN) response (17), suggesting that the IFN pathway plays a role in the host cell response against filoviruses. Both VP35 and VP24 of EBOV have been found to be involved in the IFN antagonism (6, 12, 23).

In an attempt to search for host cell antiviral proteins active against filoviruses, we analyzed the effect of the CCCH-type zinc finger antiviral protein (ZAP) (8) on EBOV and MARV replication. ZAP was discovered via its ability to inhibit Moloney murine leukemia virus (MMLV) replication (8). The cDNA of the original MMLV-resistant cell clone was derived from a Rat2 fibroblast library. The cells expressed the N-terminal part of ZAP fused to the product of the zeocin resistance gene (NZAP-Zeo) (8). Inhibition of MMLV is accompanied by a specific loss of viral mRNAs from the cytoplasm, whereas the level of RNA within the nucleus remained unimpaired (8). In addition, it was shown that NZAP-Zeo also inhibits the replication of alphaviruses by preventing translation of incoming RNA (2). Further studies demonstrated that the second and fourth zinc finger motifs of ZAP are important for inhibition of MMLV and Sindbis virus (SIN) (11). For SIN, direct binding of certain genomic RNA fragments to ZAP was described, and destabilization of the bound RNA was discussed as the mechanism of action (11). However, the expression of NZAP-Zeo does not produce a broad-spectrum antiviral state, as yellow fever virus (YFV), vesicular stomatitis virus, or poliovirus are not affected by NZAP-Zeo (2).

In the present study, we demonstrate that ZAP is also active against filoviruses, indicating that ZAP's activity is not restricted to positive-strand RNA viruses and retroviruses. The second and fourth zinc finger motifs especially were important for inhibition of filovirus replication, as shown for MMLV and SIN. The mRNA encoding the polymerase seems to be a target of ZAP.

* Corresponding author. Mailing address: Department of Virology, Bernhard-Nocht-Strasse 74, Bernhard-Nocht-Institute for Tropical Medicine, 20359 Hamburg, Germany. Phone: 49 40 42818 454. Fax: 49 40 42818 378. E-mail: kuemmerer@bni.uni-hamburg.de.

† S. Müller and P. Möller contributed equally to this paper.

‡ Present address: The Rockefeller University, 1230 York Avenue, New York, NY 10021.

§ Present address: Robert Koch-Institute, Nordufer 20, 13353 Berlin, Germany.

▽ Published ahead of print on 20 December 2006.

MATERIALS AND METHODS

Cell culture and viruses. All cells were maintained in Dulbecco's modified Eagle's medium supplemented with 10% fetal bovine serum. The Rat2-Zeo cells (named Rat2-HA-Zeo cells in reference 2), Rat2-NZAP-Zeo, and Rat2-NZAP-Zeo mutant cells (2) were kept under 100 μg of zeocin/ml (Invitrogen). The tetracycline-inducible 293TRex-ZAP cell line (11) was passaged under 200 μg of zeocin/ml. Expression of ZAP was induced with 0.5 μg doxycycline/ml (Sigma-Aldrich).

Virus stocks were produced on Vero-E6 cells. Cells were infected at a multiplicity of infection (MOI) of 0.01 for 1 h with Zaire-EBOV (Gabon strain, 2002; unpublished data), Sudan-EBOV (Uganda strain, 2000; unpublished data), MARV Musoke (Kenya, 1980), or MARV Popp (West Germany, 1967). Virus was harvested from the supernatant 7 days postinfection (p.i.). All experiments with EBOV and MARV were performed in a biosafety level 4 laboratory.

Immunofluorescence assay. Zaire-EBOV-infected cells were fixed 5 days p.i., and immunofluorescence analysis was performed using a monoclonal antibody directed against Zaire-EBOV nucleoprotein NP (MAb B6C1; dilution, 1:500; unpublished data). Bound antibodies were detected with rhodamine-labeled goat anti-mouse immunoglobulin G (dilution, 1:100) (Dianova).

Virus titration. Titration of EBOV and MARV was performed on Vero-E6 cells. The inoculum was removed after 1 h, and cells were overlaid with medium containing 0.9% methylcellulose. Five days p.i., the methylcellulose overlay was removed and cells were fixed with 4% formaldehyde in phosphate-buffered saline for at least 1 h. Plaques of MARV Popp were visualized using crystal violet staining (1% crystal violet in 20% ethanol). Infected foci of Zaire-EBOV, Sudan-EBOV, and MARV Musoke were detected by an immunofocus assay using virus-specific polyclonal antibodies raised in goats (unpublished data). Primary antibodies were diluted 1:1,000, and bound antibodies were detected with a peroxidase-conjugated rabbit anti-goat antibody (dilution, 1:250; Dianova) followed by incubation with 3,3′,5,5′-tetramethylbenzidine substrate (Mikrogen).

Real-time PCR. Isolation of viral RNA from the cell culture supernatant was performed as described previously (1). The isolated RNA from the supernatant was detected by real-time reverse transcription-PCR (RT-PCR) using the Brilliant single-step quantitative RT-PCR kit (Stratagene). For detection of EBOV RNA, the 20-μl reaction contained 2 μl of RNA, 1× RT-PCR buffer, 3 mM $MgCl_2$, 0.2 μM deoxynucleoside triphosphates, 1 U of SureStart *Taq*, 1.25 U of StrataScript reverse transcriptase, 0.4 μM of primer EBOGP-1Dfwd, 0.4 μM of primer EBOGP-1Drev, and 0.1 μM of the EBOGP-1ZPrb probe (9). The reactions were run on an ABI PRISM 7000 (Perkin Elmer) with the following steps: (i) 30 min at 42°C; (ii) 15 min at 95°C; (iii) 45 cycles, with 1 cycle consisting of 5 s at 95°C and 30 s at 58°C. For detection of MARV, 0.4 μM primer MBGGP3fwd, 0.4 μM primer MBGGP3rev, and 0.1 μM MBGGP3prb probe were used (10). In vitro transcripts of the target regions were used in the PCR to generate a standard curve for viral RNA quantification.

For quantitative analysis of viral RNA within infected cells, total cellular RNA was isolated using TRIzol (Invitrogen). Total cellular RNA (100 ng) was denatured for 5 min at 65°C in the presence of 10 nmol deoxynucleoside triphosphates and 10 pmol primer binding to mRNA, including L mRNA [oligo $(dT)_{30}$], genomic RNA (EBOV-18046 forward, 5′ GAGTTGATTAGTGTGTGCAATA GGTTTAC 3′), or antigenomic RNA (EBOV-18316 reverse, 5′ TAGATCAAT ATGATGTATGAGAGCAATTTATGAG 3′), respectively. After cooling, the mixture was complemented with 5 mM dithiothreitol (Invitrogen), 20 U RNaseOUT (Invitrogen), and 60 U SuperScript III reverse transcriptase (Invitrogen) in 1× first-strand buffer (Invitrogen) (final reaction volume of 20 μl). RT was performed for 1 h at 50°C (mRNA) or for 1 h at 55°C (genomic and antigenomic RNA). After inactivation of the reverse transcriptase for 15 min at 70°C, 2 μl of each RT reaction was used as template for quantitative real-time PCR using the QuantiTect SYBR Green PCR kit (QIAGEN). The 20-μl reaction contained 2 μl cDNA, 10 μl enzyme mix, and 10 pmol of primers EBOV-18118 forward (5′ ACCTTATATTTACATAGAATGCAGGATTCTGAAG 3′) and EBOV-18249 reverse (5′ TGCAAGTATCAGGATACTATGCACGGT 3′). The reactions were run on a LightCycler (Roche) with the following steps: (i) 15 min at 95°C and (ii) 45 cycles of 1 cycle consisting of 15 s at 94°C, 30 s at 52°C, 15 s at 72°C, and 5 s at 76°C, followed by melting curve analysis. Melting curve analysis revealed only the presence of the specific product.

Northern blot analysis. Total cellular RNA was isolated using TRIzol (Invitrogen). RNA (3 μg) was separated on a 1.5% agarose-formaldehyde gel and transferred onto a Hybond N+ membrane (Amersham Pharmacia Biotech). Primers BNI-162 (5′ GGCGCAGTCAAGTATTTGGAAG-3′) and BNI-163 (5′-TTGT AATACGACTCACTATAGGGAGTTGCTTCTCAGCCTCAGT-3′) were used to generate a Zaire-EBOV NP-specific DNA template via RT-PCR using SuperScript III reverse transcriptase. To generate an α-^{32}P-labeled riboprobe, 2 μl of the DNA template was used in a 20-μl in vitro transcription reaction mixture containing 1× transcription buffer, 25 U of T7 DNA-dependent RNA polymerase (New England BioLabs), 16 U RNaseOUT, 500 μM each of 5 mM ATP, 5 mM GTP, and 5 mM UTP, and 5 μl of [α-^{32}P]CTP (15 TBq/mmol; Hartmann Analytic GmbH). Prehybridization and hybridization were performed as described previously (13).

Western blot analysis. Cells were washed with phosphate-buffered saline and then lysed in Laemmli loading buffer (50 mM Tris-HCl, pH 6.8, 15% glycerol, 2% sodium dodecyl sulfate [SDS], 0.05% bromophenol blue, and 2% β-mercaptoethanol), sheared through a 27-gauge needle, and heated for 10 min at 90°C. Proteins were separated by SDS-polyacrylamide gel electrophoresis (PAGE). After SDS-PAGE, the proteins were transferred onto nitrocellulose membrane (Schleicher & Schuell). The membrane was stained with 2.5% fast green in 10% acetic acid for 2 min to visualize blotted proteins. Destaining was performed with 10% acetic acid for 10 min. The membrane was blocked with 10% Roti Block (Roth). For detection of ZAP, NZAP-Zeo, or NZAP-Zeo mutants, a rabbit anti-ZAP antibody (RU-893; kindly provided by M. MacDonald, Rockefeller University, New York, NY) diluted 1:1,500 was used. Detection of ZAP-hemagglutinin (HA) was performed using an anti-HA monoclonal antibody (Covance) at a dilution of 1:10,000. The EBOV NP protein was detected using a polyclonal goat serum (dilution, 1:5,000; unpublished data). For detection of glyceraldehyde-3-phosphate dehydrogenase (GAPDH), a monoclonal antibody (Ambion) was used at a dilution of 1:4,000. Peroxidase-coupled secondary antibodies directed against rabbit or mouse immunoglobulin (Pierce) were diluted 1:10,000. Peroxidase-coupled anti-goat antibody (Dianova) was diluted 1:40,000. Detection of the peroxidase-coupled antibodies was performed with Super Signal West Pico Chemiluminescent substrate (Pierce).

Artificial EBOV replicon system. Huh-T7 cells (5×10^5 in a 7-cm^2 well) were transfected with T7 RNA polymerase promoter plasmids expressing Zaire-EBOV NP (0.5 μg), L protein (1 to 4 μg), VP35 (0.5 μg), VP30 (0.1 μg) (20), a T7 promoter-driven minigenome encoding *Renilla* luciferase reporter (1 μg) (14), and plasmid pC-T7Pol (0.5 μg) (21), as described previously (3). Different amounts of plasmid pTM1-ZAP expressing HA-tagged ZAP were added to the transfection mixture. Empty vector pTM1 was used to keep the amount of transfected DNA constant. In addition, 0.5 μg pTM1-FFluc expressing firefly luciferase derived from pGL3-control (Promega) was added to normalize *Renilla* luciferase values. *Renilla* and firefly luciferase activities were determined 2 days posttransfection using the Dual-Luciferase Reporter assay system (Promega) according to the manufacturer's instructions. Replicon activity was expressed as the *Renilla*/firefly luciferase ratio.

Plasmid construction. Total cellular RNA from virus-infected cells was isolated by TRIzol (Invitrogen). Reverse transcription of the RNA was performed using SuperScript III reverse transcriptase (Invitrogen). DNA fragments were amplified with BioTherm DNA Polymerase (GeneCraft, Germany) or Phusion DNA Polymerase (Finnzymes, Finland). To map the sequences responsive to ZAP, mRNAs of Zaire-EBOV and MARV Musoke were reverse transcribed using primer pairs matching the sequences of GenBank accession number AF086833 or Z12132, respectively. The borders of the amplified genome regions (nucleotide numbers are in parentheses) for EBOV were the following: NP (56 to 3014), VP35 (3032 to 4396), VP40 (4390 to 5894), GP (5900 to 8307), VP30 (8288 to 9729), VP24 (9885 to 11518), L1 (11501 to 12367), L2 (12083 to 14020), L3 (13501 to 15501), L4 (15001 to 18271), L4/1 + 2 (15000 to 16802), L4/2 + 3 (15775 to 17610), L4/3 + 4 (16598 to 18271), L4/1 (15000 to 16007), L4/2 (15775 to 16802), L4/3 (16598 to 17610), and L4/4 (17397 to 18271); for MARV they were the following: NP (47 to 2832), VP35 (2851 to 4398), VP40 (4412 to 5807), GP (5822 to 8655), VP30 (8762 to 9998), VP24 (9990 to 11267), L1 (11282 to 13753), L2 (13249 to 15876), L3 (15218 to 17038), and L4 (16532 to 19017). Fragments derived from the YFV infectious clone pACNR/FLYF-17x (5) (kindly provided by C. M. Rice, Rockefeller University, NY) encompassed the following nucleotides (in parentheses) according to GenBank accession number X03700: YF1 (1 to 3212), YF2 (2669 to 5917), YF3 (5401 to 8608), and YF4 (8100 to 10714). Adjacent to the genome-specific sequences, primer pairs contained either an XbaI or a BamHI site. Details of the primer sequences are available on request. In addition, a SIN fragment was amplified from the infectious SIN clone pToto1101 (24) (kindly provided by C. M. Rice, Rockefeller University, NY) using primers BNI-394 (5′-GCTCTAGACCCGTCCTGTTTGGATCATTTG-3′) and BNI-395 (5′-GCTCTAGATAGGTAGATGGGTGGATGAT-3′). PCR fragments were cloned either into the XbaI site of pGL3-Control (Promega) or into the BamHI site of pGL3-B. The latter plasmid was constructed by removing the original BamHI site. In a second step, a new BamHI site was introduced next to the XbaI site by site-directed mutagenesis. Positive orientation of the inserted

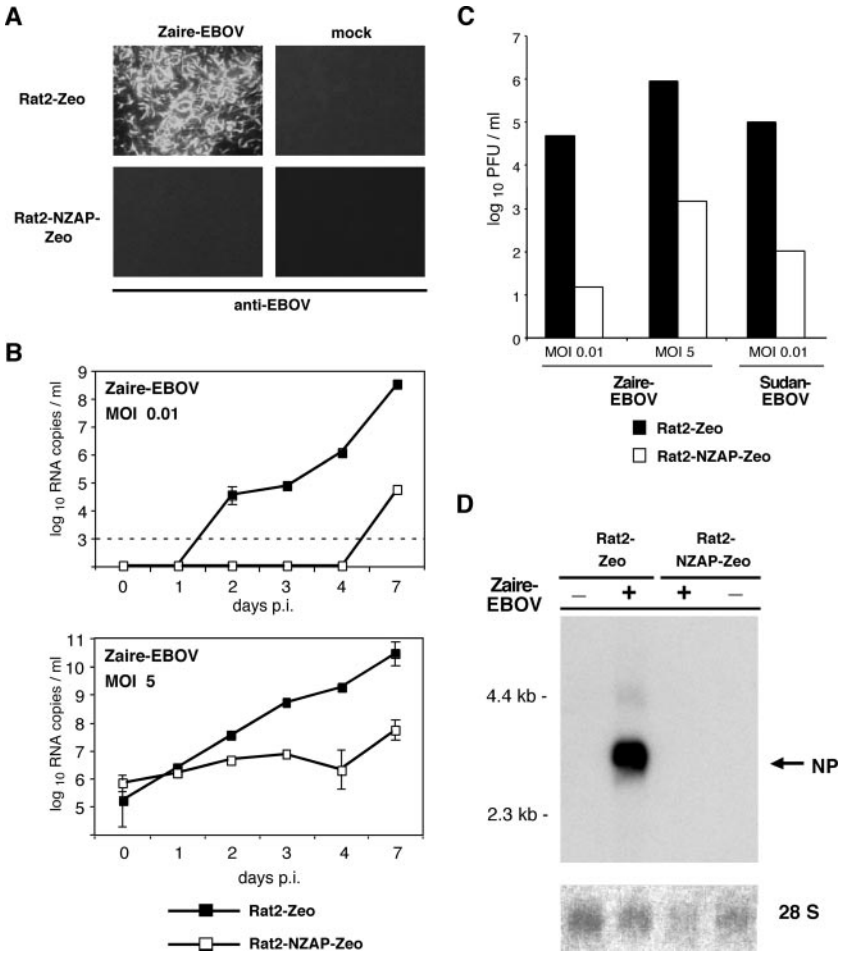

FIG. 1. Inhibition of EBOV replication in Rat2-NZAP-Zeo cells. (A) Immunofluorescence analysis of NZAP-Zeo-expressing cells infected with Zaire-EBOV. Rat2-Zeo cells expressing the empty vector or Rat2-NZAP-Zeo cells expressing the N-terminal portion of ZAP fused to the product of the zeocin resistance gene were infected with Zaire-EBOV at an MOI of 1. Five days p.i., cells were fixed and immunofluorescence analysis was performed using a monoclonal antibody directed against Zaire-EBOV NP protein. (B) Growth kinetics of Zaire-EBOV. Rat2-Zeo cells or Rat2-NZAP-Zeo cells were infected with Zaire-EBOV at an MOI of 0.01 or 5. The amount of Zaire-EBOV-specific RNA in the supernatant was quantified using a Zaire-EBOV-specific real-time RT-PCR. The data represent the means and ranges of duplicate infection experiments. Dashed line, detection limit. (C) Determination of infectious virus titer. Rat2-Zeo or Rat2-NZAP-Zeo cells were infected with Zaire-EBOV or Sudan-EBOV at an MOI of 0.01 or 5. Seven days p.i., the amount of infectious virus released into the supernatant was determined by immunofocus assay on Vero-E6 cells. (D) Northern blot analysis of Zaire-EBOV NP-specific RNA. Rat2-Zeo or Rat2-NZAP-Zeo cells were infected with Zaire-EBOV at an MOI of 1. Five days p.i., total RNA was isolated and Northern blot hybridization was performed with a ^{32}P-labeled probe directed against Zaire-EBOV NP RNA. Noninfected cells served as a control. The methylene blue-stained 28S RNA is shown below the blot as a semiquantitative marker for gel loading and RNA transfer.

sequences was verified by sequencing or digestion with suitable restriction enzymes.

Mapping of ZAP-sensitive sequences. Rat2-Zeo, Rat2-NZAP-Zeo, or Rat2-NZAP-Zeo mutant cell lines were seeded in 24-well plates at 2×10^5 cells per well. The next day, 0.4 μg of pGL3 derivatives containing virus-specific insertions and 0.1 μg of pRL-TK (Promega) was transfected in serum-free medium using 2 μl of Lipofectamine 2000 (Invitrogen). Plasmid pRL-TK is a Renilla luciferase reporter plasmid previously shown not to be sensitive to ZAP (11) which was included to normalize the firefly luciferase values. At 5 h after transfection, the medium was exchanged by Dulbecco's modified Eagle medium containing 10% serum and 100 μg zeocin/ml. At 48 h after transfection, cells were lysed and *Renilla* and firefly luciferase activities were measured using the Dual-Luciferase Reporter assay system according to the manufacturer's instructions. The level of inhibition was calculated by forming the ratio between the normalized luciferase activity expressed in empty Rat2-Zeo cells and the normalized luciferase activity in Rat2 cells expressing NZAP-Zeo or NZAP-Zeo mutants.

RESULTS

Inhibitory effect of NZAP-Zeo expression on EBOV. The effect of ZAP on EBOV replication was studied using cells stably expressing NZAP-Zeo (Rat2-NZAP-Zeo). Rat2-NZAP-Zeo cells and Rat2 control cells carrying the empty expression vector (Rat2-Zeo cells) were infected with Zaire-EBOV at an MOI of 1. First, virus growth was assessed by indirect immunofluorescence. Rat2-NZAP-Zeo cells showed no signs of Zaire-EBOV infection, whereas all control cells were infected (Fig. 1A). To quantify the effect of NZAP-Zeo on the growth of Zaire-EBOV more precisely, virus release was monitored after infection at an MOI of 0.01 and an MOI of 5 using a quantitative real-time RT-PCR assay. As shown in Fig. 1B,

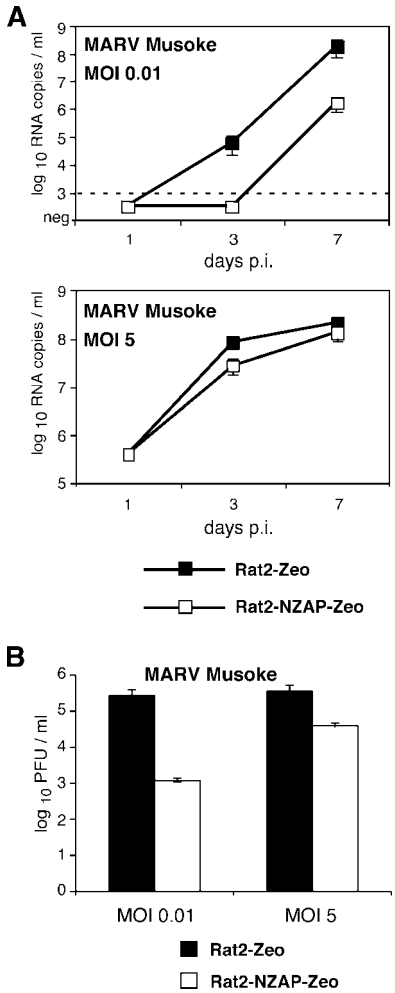

FIG. 2. Inhibition of MARV Musoke replication in Rat2-NZAP-Zeo cells. (A) Rat2-Zeo cells or Rat2-NZAP-Zeo cells were infected with MARV Musoke at an MOI of 0.01 or 5. The amount of MARV-specific RNA in the supernatant was quantified using a MARV-specific real-time RT-PCR. The data represent the means and ranges of duplicate infection experiments. Dashed line, detection limit. (B) Determination of infectious virus titer. Rat2-Zeo or Rat2-NZAP-Zeo cells were infected with MARV Musoke at an MOI of 0.01 or 5. Seven days p.i., the amount of infectious virus released into the supernatant was determined by immunofocus assay on Vero-E6 cells. The data represent the means and ranges of duplicate infection experiments. neg, negative.

expression of NZAP-Zeo resulted in a reduction of EBOV-specific RNA in the supernatant by 3 to 4 log units at both low and high MOIs. The measurement of infectious virus titer confirmed a reduction by 3 to 4 log units at day 7 postinfection (Fig. 1C). A similar level of inhibition could also be demonstrated for Sudan-EBOV after infection at an MOI of 0.01 (Fig. 1C), indicating that ZAP inhibits different EBOV subtypes.

To confirm the data on the extracellular level of EBOV RNA and infectious particles, we analyzed the intracellular level of NP-specific mRNA by Northern blotting. To this end, Rat2-Zeo and Rat2-NZAP-Zeo cells were infected with Zaire-EBOV at an MOI of 1. EBOV NP mRNA was not detectable in Rat2-NZAP-Zeo cells, while there was a strong signal in Rat2-Zeo control cells (Fig. 1D).

Effect of NZAP-Zeo expression on MARV. In view of the strong inhibitory effect of NZAP-Zeo on EBOV replication, we wondered if NZAP-Zeo also acts on viruses of the MARV genus of the filovirus family. Rat2-NZAP-Zeo and control cells were infected with MARV Musoke at an MOI of 1 and analyzed by immunofluorescence at 5 days p.i. Both cell lines showed positive fluorescence signals, indicating that MARV is not completely blocked (data not shown). However, there was a quantitative reduction in virus replication. MARV Musoke-specific RNA level in the supernatant was reduced by 2 log units after infection at an MOI of 0.01 (Fig. 2A). After infection at an MOI of 5, the released viral RNA was reduced up to 0.5 log units at an early time point (day 3 p.i.) but eventually reached the level observed for the control cells at late time points (Fig. 2A). Infectious virus titer was also reduced by 2 and 1 log units after infection at an MOI of 0.01 and an MOI of 5, respectively, at day 7 p.i. (Fig. 2B). Infection of Rat2-Zeo cells with another MARV strain (Popp) induced a severe cytopathic effect. Interestingly, expression of NZAP-Zeo largely protected the Rat2 cells from cytopathic effect (data not shown). This finding made it difficult to compare the level of virus produced by the two cell lines but suggested that NZAP-Zeo also has an antiviral effect on MARV Popp. Taken together, representatives of the MARV genus are also inhibited by NZAP-Zeo, although to a smaller extent compared to EBOV.

Inhibition of EBOV and MARV by full-length ZAP. Since Rat2-NZAP-Zeo cells express only the N-terminal part of ZAP fused with the zeocin resistance gene product, it was investigated if full-length ZAP without heterologous sequences also possesses anti-filovirus activity. For these experiments, 293TRex cells inducibly expressing full-length ZAP (293TRex-ZAP) were used. After induction of ZAP expression, cells were infected with EBOV and MARV at an MOI of 0.1. Noninduced cells served as a control. Expression of ZAP reduced the titer of Zaire-EBOV and Sudan-EBOV by 4 log units 4 days p.i. (Fig. 3A). In contrast to Rat2-Zeo cells, growth of MARV Popp did not result in a CPE in 293TRex-ZAP cells. Therefore, both MARV Musoke and MARV Popp could be included in the testing. Induction of ZAP reduced viral titers of the MARV strains by nearly 1 log unit (Fig. 3A). The expression level of ZAP in noninduced and induced cells was verified at day 4 p.i. by Western blot analysis (Fig. 3B). Taken together, these data demonstrate that the antiviral effect observed with NZAP-Zeo correspond to that of the natural ZAP gene product.

Role of zinc finger motifs of NZAP-Zeo for its antiviral activity against filoviruses. The N terminus of ZAP contains four CCCH-type zinc finger motifs. The integrity of the second and fourth zinc finger motif of ZAP is important for its antiviral effect against MMLV and SIN (11). To determine the importance of each zinc finger for inhibition of EBOV replication, cell lines expressing NZAP-Zeo variants with single mutations in each zinc finger (H86K, C88R, C168R, and H191R) (11) were infected with Zaire-EBOV and Sudan-EBOV at an MOI of 0.01. Viral titers were determined 7 days p.i. to calculate the level of inhibition for each mutant. Disruption of the second (C88R) and fourth (H191R) finger

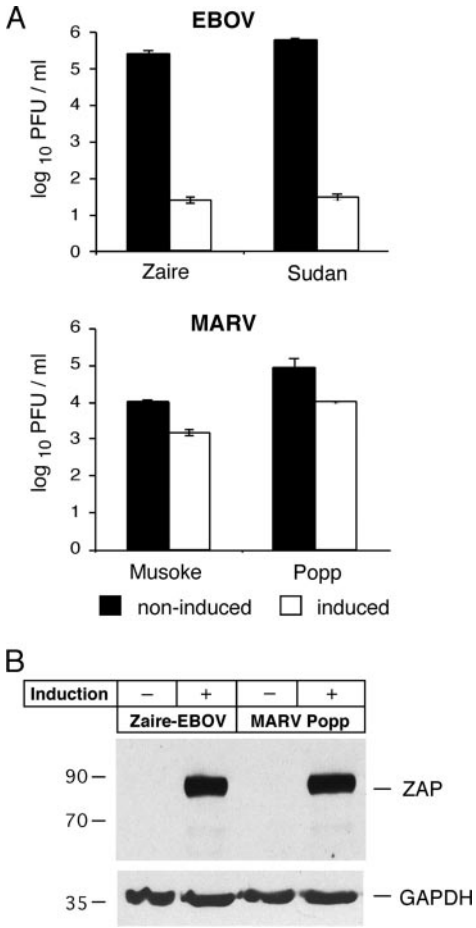

FIG. 3. Inhibition of filovirus replication in 293TRex-ZAP cells. (A) ZAP expression was induced with doxycycline in 293TRex-ZAP cells, and 6 h later cells were infected with Zaire-EBOV or Sudan-EBOV (upper panel) as well as MARV Musoke or MARV Popp (lower panel) at an MOI of 0.1. Noninduced cells served as a control. Four days p.i., the amount of infectious virus released into the supernatant was determined by immunofocus or plaque assay on Vero-E6 cells. The data represent the means and ranges of duplicate infection experiments. (B) Western blot analysis of ZAP induction in 293TRex-ZAP cells. Zaire-EBOV- and MARV Popp-infected noninduced and induced 293TRex-ZAP cells used for the experiments shown in panel A were lysed 4 days p.i. and analyzed by Western blotting. Detection of ZAP was performed using a polyclonal anti-ZAP antibody. As a loading control, GAPDH was detected using an anti-GAPDH monoclonal antibody.

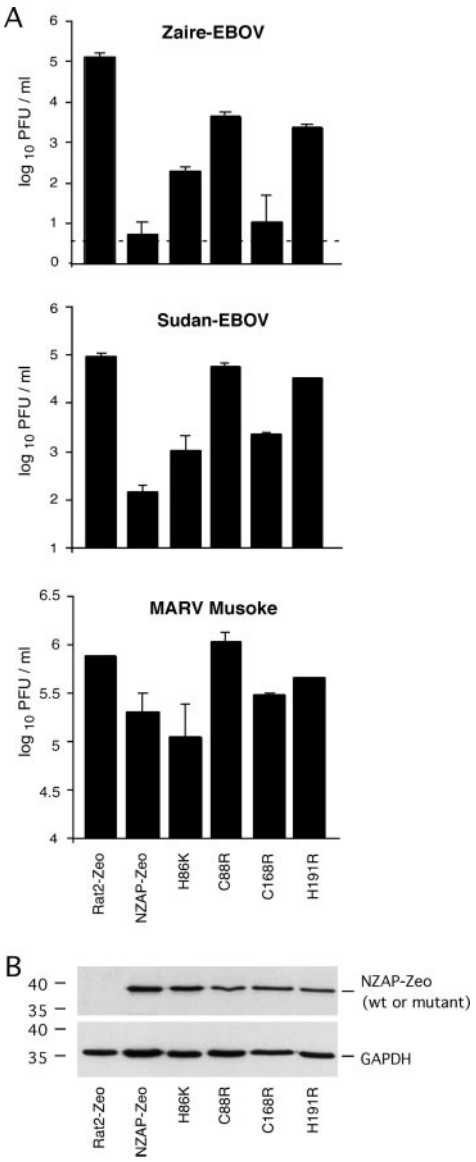

FIG. 4. Effect of mutations within the zinc finger motifs of ZAP on its antiviral activity. (A) Rat2 cells expressing wild-type NZAP-Zeo or mutants containing single amino acid exchanges (H86K, C88R, C168R, or H191R) were infected with Zaire-EBOV, Sudan-EBOV, or MARV Musoke at an MOI of 0.01. Seven days p.i., the infectious virus titer was determined by immunofocus assay. Data represent means and ranges of duplicate infection experiments. Dashed line, immunofocus assay detection limit. (B) Level of NZAP-Zeo mutant protein expressed by cell lines as detected by Western blot analysis. Rat2-Zeo cells, Rat2-NZAP-Zeo cells, and Rat2 cells expressing NZAP-Zeo mutants containing the single amino acid exchange H86K, C88R, C168R, or H191R were lysed in Laemmli loading buffer. Proteins were separated by SDS-PAGE and transferred onto a membrane. NZAP-Zeo and NZAP-Zeo mutants were detected using a polyclonal anti-ZAP antibody. As a loading control, detection of GAPDH using an anti-GAPDH monoclonal antibody was performed.

largely abolished the capability of NZAP-Zeo to inhibit growth of EBOV (Fig. 4A). The loss of inhibitory activity compared to that of wild-type NZAP-Zeo was in the range of 3 log units for both EBOV subtypes (Fig. 4A). Disruption of the first (H86K) and third (C168R) zinc finger had a lower impact on the anti-EBOV activity of NZAP-Zeo (Fig. 4A). A similar inhibition pattern was also observed for MARV Musoke, although the loss of NZAP-Zeo activity for the H191R mutant was not as dramatic as found for EBOV (Fig. 4A).

To verify that the different levels of antiviral activity are not due to different expression levels of the individual ZAP mutants, their expression levels were analyzed by Western blot analysis. As shown in Fig. 4B, all cell lines expressed comparable levels of NZAP-Zeo protein. In conclusion, the integrity of the second and fourth zinc finger motif is important for the anti-filoviral effect of NZAP-Zeo.

Mapping of EBOV and MARV sequences targeted by ZAP. Previous studies indicated that ZAP targets and destabilizes

specific genomic sequences of MMLV and SIN (11). Antiviral effects of ZAP against filoviruses may also involve reduction of virus-specific RNA. To test this hypothesis, Zaire-EBOV- and MARV Musoke-specific sequences covering all genes were cloned into a simian virus 40 (SV40) promoter-driven luciferase reporter plasmid between the 3′ end of the luciferase gene and a poly(A) signal (Fig. 5A). These constructs express fusion mRNAs containing the luciferase gene at the 5′ end and filovirus sequences at the 3′ end. Thus, targeting the filovirus sequences by ZAP will lead to reduced luciferase expression. The sequences coding for filovirus L protein were divided into four overlapping fragments (L1 to L4). Otherwise, the sequences of complete EBOV and MARV genes were tested. In addition, a SIN fragment previously shown to be sensitive to ZAP (11) was included as a positive control. The resulting plasmids were transfected into Rat2-NZAP-Zeo and control cells, and the level of RNA reduction by ZAP was calculated from the luciferase activity in cells expressing NZAP-Zeo relative to control cells (Fig. 5A). The highest level of inhibition was observed for the L4 fragments of L gene of Zaire-EBOV and MARV Musoke (Fig. 5A). Other viral sequences were also targeted, although to a smaller extent. To map potential target sequences of ZAP more precisely, the L4 fragment was divided into three overlapping fragments of about 1.8 kb in size (L4/1 + 2, L4/2 + 3, and L4/3 + 4) or into four overlapping fragments of about 1 kb in size (L4/1, L4/2, L4/3, and L4/4) (Fig. 5B). Surprisingly, luciferase expression of all three SV40 expression constructs containing 1.8-kb L fragments was inhibited to a similar extent as that observed for L4 (Fig. 5B). However, dividing the L4 fragment into 1-kb fragments resulted in the loss of ZAP-mediated inhibition, suggesting that the length of the RNA fragment is important for the effect of ZAP.

In order to demonstrate the specificity of the effect, it was tested whether YFV sequences are susceptible to ZAP in our system. It has been demonstrated previously that YFV replication is not inhibited by ZAP (2). Four overlapping fragments of about 3 kb covering the complete 11-kb YFV genome were tested in the luciferase reporter assay. As shown in Fig. 5C, the level of inhibition of all constructs was similar to that of the negative control vector pGL3. Taken together, the data of both sets of experiments indicate that sequence-specific features of

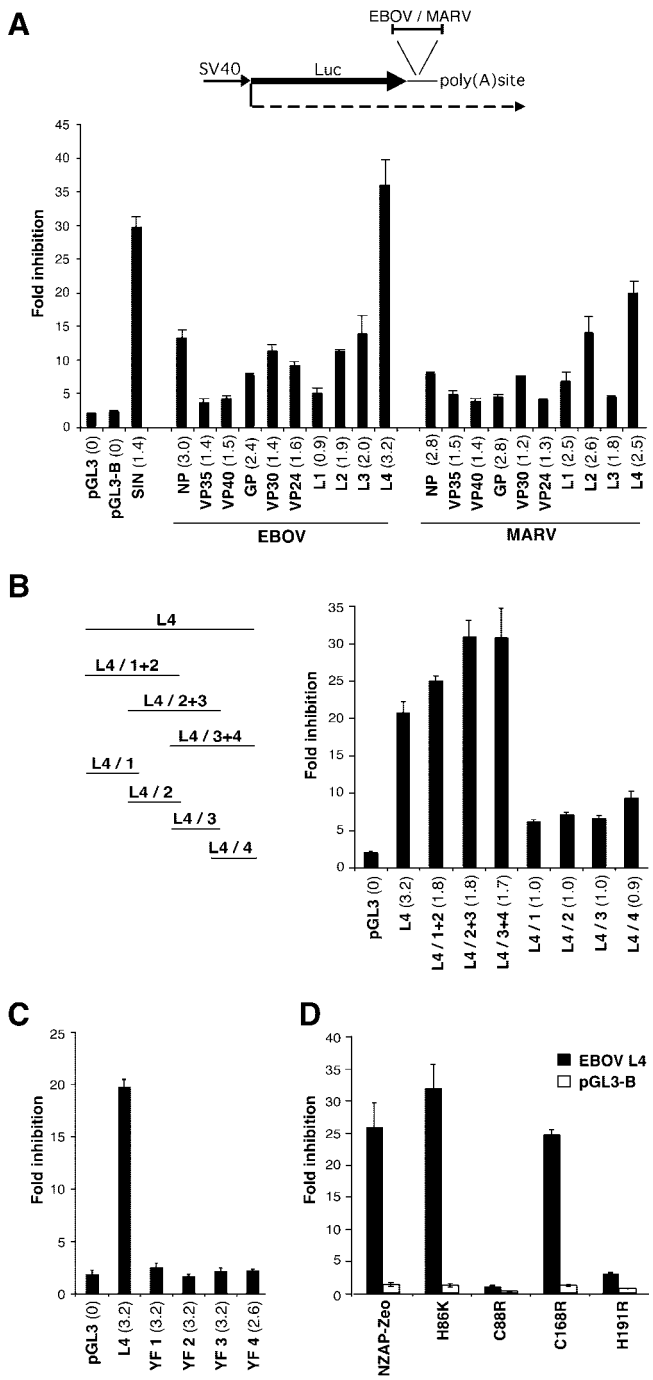

FIG. 5. Mapping of ZAP target sequences in Zaire-EBOV and MARV Musoke genomes. (A) cDNA fragments of Zaire-EBOV- and MARV Musoke-specific genes were cloned into pGL3 or pGL3-B between the firefly luciferase gene and poly(A) site. Inserted sequences as well as the approximate size of each insert (in kilobases) are indicated below each bar. The L genes were divided into four fragments (L1 to L4). SIN corresponds to a SIN genome fragment known to be sensitive to ZAP. The plasmids were transfected into Rat2-Zeo or Rat2-NZAP-Zeo cells. Cotransfection of a plasmid not sensitive to ZAP encoding *Renilla* luciferase (pRL-TK) was used to normalize firefly luciferase values. Cells were lysed 48 h posttransfection, and luciferase activity was measured. The inhibition (*n*-fold) was calculated as the normalized luciferase activity in Rat2-Zeo cells divided by the normalized luciferase activity in Rat2-NZAP-Zeo cells. Data are means and ranges of duplicate transfection experiments. (B) The EBOV L4 fragment was further divided into three or four overlapping fragments. A schematic representation of the fragments is shown at the left. Transfection and calculation of inhibition was performed as described for panel A. Numbers in brackets depict the approximate size of the inserts in kilobases. Data represent means and ranges of duplicate transfection experiments. (C) Four overlapping sequences covering the genome of YFV (YF1 to YF4) were inserted into pGL-3. The size of each insert (in kilobases) is shown in brackets. Transfection and calculation of inhibition was performed as described for panel A. Data represent means and ranges of duplicate transfection experiments. (D) The pGL-3 plasmid containing the EBOV L4 fragment was used to analyze the activity of NZAP-Zeo zinc finger mutants in the luciferase reporter assay. Transfection was performed with Rat2 cells expressing NZAP-Zeo mutants (H86K, C88R, C168R, or H191R). Empty pGL3 was used as a control. Transfection and calculation of inhibition was performed as described for panel A. Data represent means and ranges of duplicate transfection experiments.

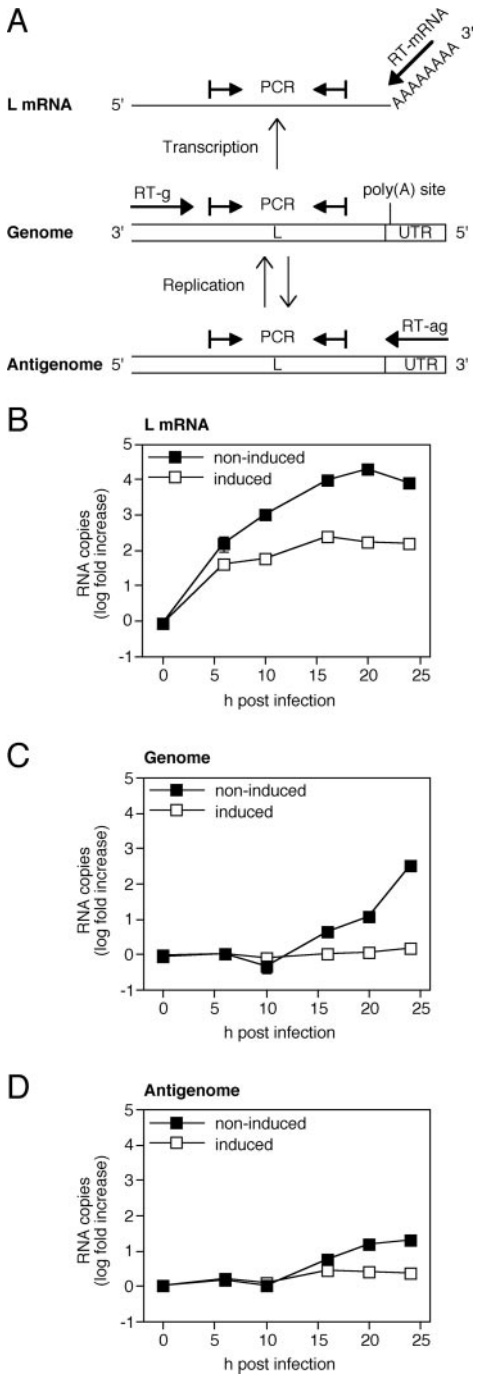

FIG. 6. Effect of ZAP on levels of L mRNA, genomic RNA, and antigenomic RNA during Zaire-EBOV infection. (A) Experimental strategy for quantification of Zaire-EBOV L mRNA, genomic RNA, and antigenomic RNA. Reverse transcription was performed with primers (large arrows) specifically binding either mRNA (RT-mRNA), genomic RNA (RT-g), or antigenomic RNA (RT-ag). The synthesized cDNA was quantified by real-time PCR using primers targeting the 3′ end of the L gene (small arrows). UTR, untranslated region; L, L gene. (B to D) 293TRex-ZAP cells were infected with Zaire-EBOV at an MOI of 3 for 1 h. After removing the inoculum, cells were induced with doxycycline. Noninduced cells served as controls. Total cellular RNA was isolated at various time points p.i. Zaire-EBOV-specific L mRNA (B), genomic RNA (C), and antigenomic RNA (D) were quantified using the PCR method as described for panel A. The amount of RNA derived from the inoculum (0 h) was defined as 1 (0 after log transformation). The average cyclic threshold (C_t) values at 0 h were the following: L mRNA, $C_t = 29$; genome, $C_t = 22$; antigenome, $C_t = 26$. Control reactions lacking reverse transcriptase were negative in the real-time PCR (data not shown). Data represent means and ranges of duplicate infection experiments (most error bars are obscured by the symbols).

the inserted fragment rather than its size per se are relevant to mediate the effect of ZAP.

To test if the integrity of the zinc fingers is important for the effect of ZAP on the EBOV L4 fragment, the SV40 promoter construct containing this fragment was transfected into the Rat2 cell lines expressing NZAP-Zeo mutants. As shown in Fig. 5D, ZAP lost its destabilizing effect on the L4 fragment if the second and fourth zinc finger motif was mutated (C88R and C168R mutant cell lines, respectively). In conclusion, the inhibitory effect of ZAP on EBOV replication in cell culture correlates with its ability to interfere with expression of mRNA containing EBOV L4 sequence.

Effect of ZAP on L mRNA level during EBOV infection. To provide evidence that L mRNA is a target for ZAP in the natural context of a virus infection, the levels of L-gene-specific mRNA as well as genomic and antigenomic RNAs were monitored during viral infection. To this end, 293TRex-ZAP cells were infected with Zaire-EBOV at an MOI of 3. ZAP expression was induced 1 h following inoculation to exclude potential interference of ZAP with virus entry. Total cellular RNA was isolated from induced and noninduced cells at different time points after infection. The RNA was reverse transcribed with primers specifically binding to either mRNA (including L mRNA), genomic RNA, or antigenomic RNA (Fig. 6A). The levels of the three different cDNAs were determined using a real-time PCR assay targeting the 3′ end of the L gene (Fig. 6A). All three RNA species were reduced in induced versus noninduced cells between 16 h and 24 h after infection. Importantly, L mRNA levels were already reduced by up to 1 log unit in ZAP-expressing cells at 6 h and 10 h after infection (Fig. 6B), while there was no evidence for an effect of ZAP on the level of genomic and antigenomic RNA at this time (Fig. 6C and D). These data indicate that ZAP interferes with L mRNA synthesis or stability during natural infection. Since the level of genomic RNA was not yet affected at early time points, the effect cannot be mediated by a reduction of the transcriptional template of L mRNA. Reduction of genome and antigenome at a later phase might be due to reduced expression of L mRNA, and thus L protein, or due to additional effects of ZAP on genome replication.

Inhibition of EBOV replicon system by ZAP and effect of L protein overexpression. Replication and transcription of an artificial EBOV minigenome is dependent on the expression of NP, L protein, VP35, and VP30. ZAP expression is expected to inhibit replicon activity if it reduces the L mRNA level or affects other steps of EBOV replication and gene expression. To test this hypothesis, expression plasmids for NP, L protein, VP35, VP30, and an EBOV-specific minigenome expressing *Renilla* luciferase as a reporter were cotransfected with increasing amounts of a plasmid expressing HA-tagged ZAP. pTM1-FFluc expressing firefly luciferase was included to correct for

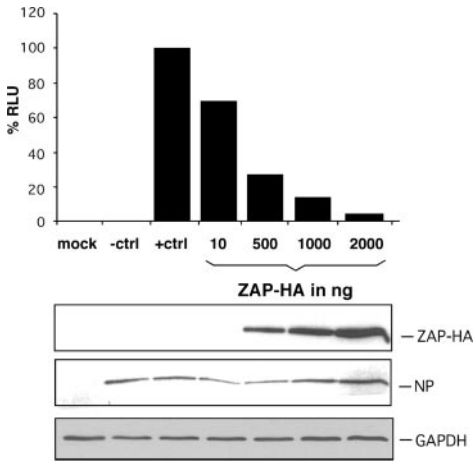

FIG. 7. Inhibition of Zaire-EBOV replicon system by ZAP. Huh-T7 cells were transfected with plasmids encoding Zaire-EBOV NP, L protein, VP35, VP30, and minigenome containing a *Renilla* luciferase gene. Increasing amounts of plasmid encoding ZAP-HA were cotransfected as indicated (−ctrl, negative control without L plasmid; +ctrl, positive control without ZAP-HA plasmid). Empty vector pTM1 was used to keep the amount of transfected DNA constant. Plasmid pTM1-FFluc was included to normalize *Renilla* luciferase values. Luciferase activities were determined 2 days posttransfection. The expression levels of ZAP-HA and EBOV NP were analyzed by Western blot using anti-HA monoclonal antibody and anti-Zaire-EBOV polyclonal antibody, respectively (bottom). The amount of cell lysate loaded on the protein gel was adjusted according to the firefly luciferase values to ensure comparability with the normalized *Renilla* values. The levels of GAPDH served as a loading control.

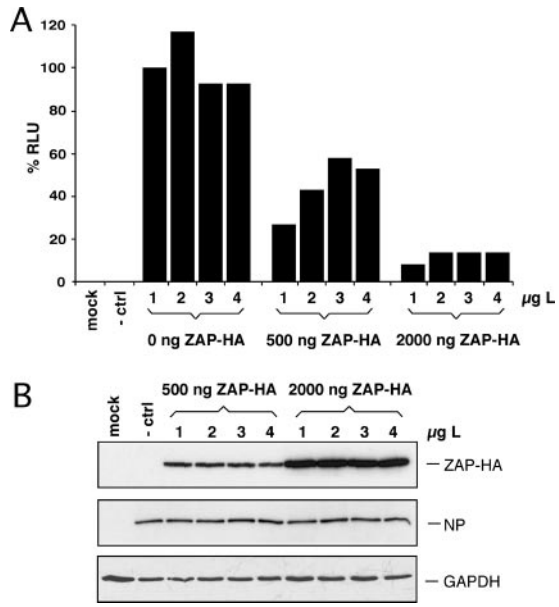

FIG. 8. Effect of L-protein overexpression on ZAP-induced inhibition of the Zaire-EBOV replicon system. (A) Huh-T7 cells were transfected with plasmids encoding Zaire-EBOV NP, VP35, VP30, increasing amounts of L-protein expression plasmid, and a minigenome containing a *Renilla* luciferase gene (−ctrl, negative control without L plasmid). Different amounts of ZAP-HA expression plasmid were cotransfected. Empty vector pTM1 was used to keep the amount of transfected DNA constant. Plasmid pTM1-FFluc was included to normalize *Renilla* luciferase values. (B) Expression levels of ZAP-HA and EBOV NP were analyzed by Western blot using anti-HA monoclonal antibody and anti-Zaire-EBOV polyclonal antibody, respectively. The amount of cell lysate loaded on the protein gel was adjusted according to the firefly luciferase values to ensure comparability with the normalized *Renilla* values. The levels of GAPDH served as a loading control.

variation in transfection efficacy and unspecific effects of ZAP. Firefly and *Renilla* luciferase activities were measured 2 days posttransfection. As little as 10 ng of ZAP-expressing plasmid was sufficient to reduce reporter gene expression by 30% (Fig. 7). Increasing the amount of ZAP reduced the replicon activity by up to 95%, while there was no major change in NP level as measured by Western blot analysis (Fig. 7).

If decreased expression of L protein was indeed involved in reduced luciferase expression by the minigenome, it might be possible to rescue replicon activity by increasing the amount of L protein in the cell. To this end, the amount of L protein expression plasmid in the transfection mixture was increased stepwise from 1 μg to 4 μg. The replicon components were transfected in the absence of ZAP or in the presence of 0.5 μg or 2 μg ZAP expression plasmid (Fig. 8A). Increasing the amount of L protein expression plasmid had no effect on ZAP expression, as demonstrated by Western blot analysis (Fig. 8B). In the absence of ZAP, luciferase gene expression was not changed by increased L protein levels (Fig. 8A). However, if the replicon was suppressed by cotransfection of 0.5 μg ZAP expression plasmid, overexpression of L protein increased replicon activity about twofold (Fig. 8A). A similar partial rescue effect was seen if 2 μg ZAP expression plasmid was transfected. In both experiments, a saturation effect was observed upon transfection of ≥3 μg L protein plasmid, suggesting that ZAP exerts additional inhibitory effects that are not related to L protein expression. Western blot analysis demonstrates that at least NP expression is not affected by ZAP (Fig. 8B). In conclusion, the experiments indicate that increased levels of L protein can partially compensate for the inhibitory effect of ZAP on replicon activity, which is consistent with the observation that ZAP reduces the L mRNA level during natural infection.

DISCUSSION

This study provides evidence that ZAP has an antiviral effect against EBOV and MARV in cell culture. The growth of Zaire-EBOV and Sudan-EBOV was inhibited by several orders of magnitude. The antiviral effect against MARV was less pronounced, suggesting that the degree of inhibition is dependent on the filovirus species. Similar observations have been made for members of the alphavirus genus. While SIN was strongly inhibited by 3 to 8 log units, NZAP-Zeo expression affected replication of Semliki Forest virus and Ross River virus to a lesser degree (2). Taking these data together, it seems that ZAP is active against various members within one virus family, although to different levels. Furthermore, our data demonstrate that the activity of ZAP is not restricted to plus-strand RNA viruses and retroviruses.

As described for MMLV and SIN, the second and fourth zinc finger motifs particularly were important for the antifiloviral effect. This finding suggests that the mechanism of action is similar for plus- and negative-strand RNA viruses,

although the precise mechanism is not known. The fact that RNA viruses replicating solely in the cytoplasm are affected suggests that ZAP exerts its effects in the cytoplasm. Consistent with this speculation, specific reduction of the cytoplasmic viral RNA levels of MMLV (8) and inhibition of translation of incoming SIN RNA have been described (2). Further studies indicated that specific regions within the MMLV and SIN genomes are targeted by ZAP, leading to destabilization of the respective viral RNAs (11). Using the same assay as has been used in these studies, we identified a 3.2-kb sequence within the L gene of EBOV and a 2.5-kb sequence within the L gene of MARV to be sensitive to ZAP. The precise target region on EBOV RNA could not be mapped, since all 1.8-kb subfragments appeared to be targeted by ZAP, suggesting that the L4 fragment contains several target sites. However, reducing the fragment size to 1 kb resulted in a drastic loss of inhibition, indicating that a minimum sequence length is required for interaction with ZAP. On the other hand, the control experiments with the long YFV sequences indicate that the inhibition observed in the luciferase reporter assay does not simply correlate with the size of the inserted fragment. The precise mechanism of interaction of ZAP with the L-gene sequences is not clear. Guo et al. showed that ZAP directly binds to SIN RNA (11). We assume that the effect seen with filovirus sequences also stems from destabilization of virus RNA, although the data do not exclude a role of ZAP at the level of RNA transcription or translation. The observations that ZAP is active in three different expression systems, i.e., (i) in an SV40 expression system, which is dependent on cellular RNA polymerase II; (ii) in the context of viral infection, where mRNA synthesis is dependent on the viral RNA polymerase; and (iii) in an artificial replicon system, where mRNA synthesis is driven by T7 RNA polymerase, do not argue for an effect of ZAP on promoter or RNA polymerase.

In addition to the luciferase gene-L mRNA fusion experiments, two lines of evidence suggest that L mRNA is a target of ZAP. First, L mRNA was reduced early after EBOV infection when the level of genomic RNA still corresponded to that of the inoculum. This largely excludes that the reduction of L mRNA is due to degradation of its transcriptional template. Synthesis of antigenomic RNA, which shares the L gene sequence with the L mRNA, was also reduced in cells expressing ZAP. However, the synthesis of new antigenomic RNA initiated later than that of L mRNA. Therefore, it cannot be distinguished if the antigenomic RNA is also a target for ZAP or if its decrease is a result of reduced synthesis of L protein. It might be that ZAP is not acting on antigenomic RNA, as it is encapsidated by the NP. The second observation arguing for an interference of ZAP with L gene expression, presumably at the level of mRNA, was that the inhibitory effect of ZAP in the artificial replicon system could be partially compensated for by overexpression of L protein. The partial nature of the rescue effect suggests that there exist additional targets of ZAP.

The data obtained with the artificial replicon system also indicate that transiently expressed ZAP is functional. Thus, vector-driven expression of ZAP might be a tool to downregulate filovirus replication. Alternatively, upregulation of endogenous ZAP could have a protective or therapeutic effect. The gene encoding human ZAP is localized on chromosome 7 (Ensembl Gene ID ENSG00000105939). Two isoforms of about 100 and 77 kDa in size exist, probably representing two splice variants. Further studies will elucidate if human ZAP is active against filoviruses and plays a role in the innate response of humans.

ACKNOWLEDGMENTS

We thank Angelika Lander for expert technical assistance. We thank Margaret MacDonald and Guangxia Gao for providing plasmids pBabe-Haz, pBabe-NZAP-Zeo (wild-type and zinc finger mutants), Rat2-Zeo cells, Rat2-NZAP-Zeo cells (wild-type and zinc finger mutants), and 293TRex-ZAP cells; V. Gauss-Müller for providing the Huh-T7 cells; C. M. Rice for providing plasmids pToto1101 and pACNR/FLYF-17x; T. Takimoto and Y. Kawaoka for the plasmid pC-T7Pol; and Christian Drosten for critical reading of the manuscript.

This work was supported by the Deutsche Forschungsgemeinschaft, Sonderforschungsbereich 535 TP A13 and 593 TP B3, and by the Land Hessen through a fellowship to Peggy Möller. The Bernhard-Nocht-Institute is supported by the Bundesministerium für Gesundheit and the Freie und Hansestadt Hamburg.

REFERENCES

1. **Asper, M., T. Sternsdorf, M. Hass, C. Drosten, A. Rhode, H. Schmitz, and S. Günther.** 2004. Inhibition of different Lassa virus strains by alpha and gamma interferons and comparison with a less pathogenic arenavirus. J. Virol. **78:**3162–3169.
2. **Bick, M. J., J. W. Carroll, G. Gao, S. P. Goff, C. M. Rice, and M. R. MacDonald.** 2003. Expression of the zinc-finger antiviral protein inhibits alphavirus replication. J. Virol. **77:**11555–11562.
3. **Boehmann, Y., S. Enterlein, A. Randolf, and E. Mühlberger.** 2005. A reconstituted replication and transcription system for Ebola virus Reston and comparison with Ebola virus Zaire. Virology **332:**406–417.
4. **Bowen, E. T., G. Lloyd, W. J. Harris, G. S. Platt, A. Baskerville, and E. E. Vella.** 1977. Viral haemorrhagic fever in southern Sudan and northern Zaire. Preliminary studies on the aetiological agent. Lancet **i:**571–573.
5. **Bredenbeek, P. J., E. A. Kooi, B. Lindenbach, N. Huijkman, C. M. Rice, and W. J. Spaan.** 2003. A stable full-length yellow fever virus cDNA clone and the role of conserved RNA elements in flavivirus replication. J. Gen. Virol. **84:**1261–1268.
6. **Cardenas, W. B., Y. M. Loo, M. Gale, Jr., A. L. Hartman, C. R. Kimberlin, L. Martinez-Sobrido, E. O. Saphire, and C. F. Basler.** 2006. Ebola virus VP35 protein binds double-stranded RNA and inhibits alpha/beta interferon production induced by RIG-I signaling. J. Virol. **80:**5168–5178.
7. **Dolnik, O., V. Volchkova, W. Garten, C. Carbonnelle, S. Becker, J. Kahnt, U. Stroher, H. D. Klenk, and V. Volchkov.** 2004. Ectodomain shedding of the glycoprotein GP of Ebola virus. EMBO J. **23:**2175–2184.
8. **Gao, G., X. Guo, and S. P. Goff.** 2002. Inhibition of retroviral RNA production by ZAP, a CCCH-type zinc finger protein. Science **297:**1703–1706.
9. **Gibb, T. R., D. A. Norwood, Jr., N. Woollen, and E. A. Henchal.** 2001. Development and evaluation of a fluorogenic 5′ nuclease assay to detect and differentiate between Ebola virus subtypes Zaire and Sudan. J. Clin. Microbiol. **39:**4125–4130.
10. **Gibb, T. R., D. A. Norwood, Jr., N. Woollen, and E. A. Henchal.** 2001. Development and evaluation of a fluorogenic 5′-nuclease assay to identify Marburg virus. Mol. Cell Probes. **15:**259–266.
11. **Guo, X., J. W. Carroll, M. R. MacDonald, S. P. Goff, and G. Gao.** 2004. The zinc finger antiviral protein directly binds to specific viral mRNAs through the CCCH zinc finger motifs. J. Virol. **78:**12781–12787.
12. **Hartman, A. L., J. S. Towner, and S. T. Nichol.** 2004. A C-terminal basic amino acid motif of Zaire ebolavirus VP35 is essential for type I interferon antagonism and displays high identity with the RNA-binding domain of another interferon antagonist, the NS1 protein of influenza A virus. Virology **328:**177–184.
13. **Hass, M., U. Golnitz, S. Müller, B. Becker-Ziaja, and S. Günther.** 2004. Replicon system for Lassa virus. J. Virol. **78:**13793–13803.
14. **Hoenen, T., A. Groseth, L. Kolesnikova, S. Theriault, H. Ebihara, B. Hartlieb, S. Bamberg, H. Feldmann, U. Stroher, and S. Becker.** 2006. Infection of naive target cells with virus-like particles: implications for the function of Ebola virus VP24. J. Virol. **80:**7260–7264.
15. **Hoenen, T., V. Volchkov, L. Kolesnikova, E. Mittler, J. Timmins, M. Ottmann, O. Reynard, S. Becker, and W. Weissenhorn.** 2005. VP40 octamers are essential for Ebola virus replication. J. Virol. **79:**1898–1905.
16. **Huang, Y., L. Xu, Y. Sun, and G. J. Nabel.** 2002. The assembly of Ebola virus nucleocapsid requires virion-associated proteins 35 and 24 and posttranslational modification of nucleoprotein. Mol. Cell. **10:**307–316.
17. **Kash, J. C., E. Mühlberger, V. Carter, M. Grosch, O. Perwitasari, S. C. Proll, M. J. Thomas, F. Weber, H. D. Klenk, and M. G. Katze.** 2006. Global suppression of the host antiviral response by Ebola and Marburg viruses:

increased antagonism of the type I interferon response is associated with enhanced virulence. J. Virol. **80:**3009–3020.

18. **Kolesnikova, L., S. Bamberg, B. Berghofer, and S. Becker.** 2004. The matrix protein of Marburg virus is transported to the plasma membrane along cellular membranes: exploiting the retrograde late endosomal pathway. J. Virol. **78:**2382–2393.
19. **Martini, G. A., and R. Siegert.** 1971. Marburg virus disease. Springer Verlag, Berlin, Germany.
20. **Mühlberger, E., M. Weik, V. E. Volchkov, H. D. Klenk, and S. Becker.** 1999. Comparison of the transcription and replication strategies of Marburg virus and Ebola virus by using artificial replication systems. J. Virol. **73:**2333–2342.
21. **Neumann, G., H. Feldmann, S. Watanabe, I. Lukashevich, and Y. Kawaoka.** 2002. Reverse genetics demonstrates that proteolytic processing of the Ebola virus glycoprotein is not essential for replication in cell culture. J. Virol. **76:**406–410.
22. **Piot, P., P. Sureau, J. G. Breman, D. L. Heymann, V. Kintoki, M. Masamba, M. Mbuyi, M. Miatudila, J. F. Ruppol, S. van Nieuwenhove, M. K. White, G. van der Groen, P. A. Webb, H. Wulff, and K. M. Johnson.** 1976. Clinical aspects of Ebola virus infection in Yambuku Area, Zaire, p. 7–14. *In* S. R. Pattyn (ed.), Ebola virus haemorrhagic fever. Elsevier/North-Holland, Amsterdam, The Netherlands.
23. **Reid, S. P., L. W. Leung, A. L. Hartman, O. Martinez, M. L. Shaw, C. Carbonnelle, V. E. Volchkov, S. T. Nichol, and C. F. Basler.** 2006. Ebola virus VP24 binds karyopherin alpha1 and blocks STAT1 nuclear accumulation. J. Virol. **80:**5156–5167.
24. **Rice, C. M., R. Levis, J. H. Strauss, and H. V. Huang.** 1987. Production of infectious RNA transcripts from Sindbis virus cDNA clones: mapping of lethal mutations, rescue of a temperature-sensitive marker, and in vitro mutagenesis to generate defined mutants. J. Virol. **61:**3809–3819.
25. **Sanchez, A., A. S. Khan, S. R. Zaki, G. J. Nabel, T. G. Ksiazek, and C. J. Peters.** 2001. *Filoviridae*: Marburg and Ebola viruses, p. 1279–1304. *In* D. M. Knipe and P. M. Howley (ed.), Fields virology, 4th ed., vol. 1. Lippincott-Raven Publishers, Philadelphia, PA.